

SSDA-YOLO: SEMI-SUPERVISED DOMAIN ADAPTIVE YOLO FOR CROSS-DOMAIN OBJECT DETECTION

Huayi Zhou^{*} Fei Jiang[†] Hongtao Lu^{*}

^{*} Shanghai Jiao Tong University, sjtu_zhy@sjtu.edu.cn, htlu@sjtu.edu.cn;

[†] East China Normal University, fjiang@mail.ecnu.edu.cn

ABSTRACT

Domain adaptive object detection (DAOD) aims to alleviate transfer performance degradation caused by the cross-domain discrepancy. However, most existing DAOD methods are dominated by computationally intensive two-stage detectors, which are not the first choice for industrial applications. In this paper, we propose a novel semi-supervised domain adaptive YOLO (SSDA-YOLO) based method to improve cross-domain detection performance by integrating the compact one-stage detector YOLOv5 with domain adaptation. Specifically, we adapt the knowledge distillation framework with the Mean Teacher model to assist the student model in obtaining instance-level features of the unlabeled target domain. We also utilize the scene style transfer to cross-generate pseudo images in different domains for remedying image-level differences. In addition, an intuitive consistency loss is proposed to further align cross-domain predictions. We evaluate our proposed SSDA-YOLO on public benchmarks including PascalVOC, Clipart1k, Cityscapes, and Foggy Cityscapes. Moreover, to verify its generalization, we conduct experiments on yawning detection datasets collected from various classrooms. The results show considerable improvements of our method in these DAOD tasks. Our code is available on <https://github.com/hnuzhy/SSDA-YOLO>.

Index Terms— Domain adaptation, knowledge distillation, semi-supervised, YOLO.

1. INTRODUCTION

Modern object detection methods based on convolution neural networks (CNNs) have achieved many remarkable improvements [1, 2, 3, 4, 5, 6, 7]. However, the high accuracy of these methods are mostly restricted to the training set source domain. Thus, even if state-of-the-art methods achieve superb results on large scale benchmarks (e.g., PascalVOC [8], MSCOCO [9], and OpenImages [10]), significant performance degradation often arises when testing under the very different target domain scenario. The new target scene may include dissimilar image styles, lighting conditions, image quality, camera perspectives, etc., which often bring considerable domain shifts between the training and test data.

Although collecting more training data can alleviate this problem, it is impractical for the expensive and time-consuming labeling process. In some scenarios, e.g. biomedical image, it is even impossible to get extensive precise annotations.

Addressing the domain gap between source training datasets and target testing datasets is the focus of domain adaptive object detection (DAOD) [11, 12, 13, 14, 15, 16]. Generally, the DAOD attempts to learn a robust and generalizable detector using labeled data from the source domain and unlabeled data from the target domain. The domain adaptive Faster R-CNN [11] is a milestone study developed for tackling the domain shift problem in object detection. Following [11], most domain adaptation approaches [12, 13, 14, 15, 16] are still based on the Faster R-CNN [1]. Instead of using the two-stage detector Faster R-CNN with ROIs for more convenient local adaptation, some recent works [17, 18, 16, 19] have proposed one-stage detector based methods considering its computational advantage. Following YOLO series [20, 6, 21], some more light-weight DAOD methods are proposed [22, 23, 24, 25]. Generally, the particular domain adaptive solution is inseparable from the breakthrough in object detection methods and architectures.

Towards resource-limited and time-critical real applications, we adopt the current widely used YOLOv5 [21] as the basic object detector in our framework. There are two actualities motivate us. On one hand, one-stage object detectors, YOLO series particularly (e.g., YOLOv5 [21] and YOLOX [7]), can reach almost real-time with maintaining comparable accuracy as two-stage detectors. This makes them invaluable for time-sensitive scenes like autonomous driving and action recognition. On the other hand, two-stage Faster R-CNN based methods have dominated the DAOD field. Although YOLOv5 has shown a compelling balance of high performance and time-consuming currently, few researches explore the introduction of the YOLO architecture. Thus, we expect to excavate and migrate the superiority of YOLOv5 in DAOD.

In this paper, we propose a novel semi-supervised domain adaptive YOLO (SSDA-YOLO) method. With the YOLOv5 as the backbone network, SSDA-YOLO can extract source domain features efficiently by fully supervised learning. In order to obtain *instance-level* features of the target

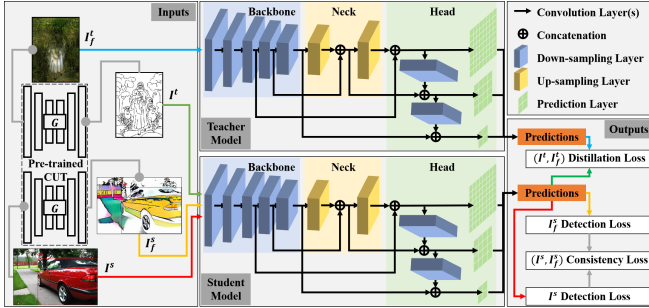


Fig. 1. The overall architecture of our proposed SSDA-YOLO. **Middle:** We adopt the original YOLOv5 [21] network as the basic detector for both teacher and student models in a knowledge distillation framework. **Left:** Besides taking the real source image I^s and target image I^t as inputs during training, we have also generated the target-like fake source image I_f^s and the source-like fake target image I_f^t using corresponding pre-trained CUT [27] models to alleviate image-level domain differences. **Right:** Based on predictions of multiple inputs (with different colors), we have constructed corresponding loss functions for supporting the semi-supervised learning.

domain, we adopt the knowledge distillation framework, and use the Mean Teacher [26] guided teacher network to detect unlabeled target images. Then, we filter the predictions to generate strong pseudo-labels iteratively for enforcing a relatively unbiased updating of the student network. Furthermore, to narrow the distance between the teacher and student model in *image-level*, we use the unpaired image generation approach CUT [27] to synthesize pseudo images offline as additional inputs. The overall architecture is shown in Fig. 1. To verify the effectiveness of SSDA-YOLO in DAOD tasks, we have conducted extensive experiments using both public benchmarks and yawning detection datasets extracted from real classroom scenarios. Experiment results show significant improvements on each target domain test set.

In summary, our contributions are as follows: 1) We propose a novel semi-supervised domain adaptive YOLO (SSDA-YOLO) for tackling the DAOD problem, which combines the one-stage detector with a knowledge distillation framework. 2) Two newly designed domain adaptive penalty functions including the distillation loss and the consistency loss are proven reasonable and effective. 3) Our method can achieve comparable or superior accuracy improvements on two popular domain transfer experiments (e.g., **PascalVOC**→**Clipart1k**, and **Cityscapes**→**Foggy Cityscapes**), and maintain appreciable generalization in yawning detection under different classroom scenarios.

2. RELATED WORKS

2.1. Object Detection

Modern object detection methods can be grouped into two categories: 1) The *two-stage* architectures (e.g., Faster R-CNN [1] and Mask R-CNN [4]), that first extract regions of interest (ROIs) and then operate bounding boxes classification and regression; and 2) *one-stage* detectors (e.g., SSD [3], FPN [5], FCOS [2], and YOLO series [20, 6, 21, 7]), that directly output bounding boxes and classes from the predicted feature maps with pre-defined anchors. While the former yields slightly higher accuracy, the latter is faster and more compact, which makes them better suited for time-sensitive applications and computation limited edge devices. Recently, benefits from the Cross-Stage-Partial (CSP) bottlenecks [28] and optimizations in training tricks, the one-stage YOLO series even surpass the two-stage ones both in accuracy and efficiency. In particular, we choose the YOLOv5, which combines CSPNet [28], FPN [5] and Focal loss [29], as our basic detector. Beyond that, it is proven having effective data augmentations (e.g., Mosaic and MixUp) and strong versatility during training.

2.2. Cross-Domain Object Detection

Existing cross-domain object detection methods have exclusively focused on the two-stage detector Faster R-CNN [11, 12, 14, 13, 15, 16, 30, 31, 19, 32]. Following the pioneering DA-Faster [11] which introduces the Gradient Reversal Layer (GRL) [33] and firstly designs instance-level and image-level alignments to promote performance on new domains, SWDA [12] proposes similar strong local and weak global feature alignments for improvement. Then, NLDA [14] formulates a robust learning as training with noisy labels on the target domain. UMT [13] generates fake training images using CycleGAN [34] to alleviate domain bias. Focusing on labeled data from multiple source domains, MSDA [15] proposes the Divide-and-Merge Spindle Network (DMSN) to enhance domain invariance and preserve discriminative power. SIGMA [16] represents the source and target data as graphs, and reformulates the adaptation as a graph matching problem. In comparison, some recent works try to tackle the DAOD problem using one-stage detectors [17, 18, 23, 24, 25]. For example, EPMDA [17] adapts FCOS [2] to explicitly extracts objectness maps. I³Net [18] introduces complementary modules specifically designed for the SSD [3] architecture. And [22, 24, 25] have designed pertinent methods and frameworks based on YOLOv3/4/5 respectively.

In general, DAOD is overwhelmingly dominated by the two-stage Faster R-CNN, which contains region proposals for most methods to effortlessly perform local adaptation. This has been shown to significantly improve the adaptation effectiveness. Nevertheless, on the premise of maintaining accuracy, the one-stage detector with lighter weight and faster

speed is friendly to industrial applications. Therefore, we choose to improve the one-stage detector based DAOD task. Inspired by previous methods, our proposed SSDA-YOLO adopts the YOLOv5 as backbone, and applies generative adversarial network (GAN) based CUT [27] for representative cross-domain images generation.

2.3. Semi-supervised Domain Adaptation

Unsupervised domain adaptation (UDA) is defined to adapt a model from the labeled source domain to an unlabeled target domain. It is first widely studied for image classification tasks [35, 36, 37, 38, 39]. For the DAOD problem in this paper, by default, labels of the target domain are invisible during training, but only images are used. Generally, in order to learn domain-invariant representations and minimize the distance metric among domains, almost all previous DAOD methods [11, 12, 17, 18, 16, 30, 19] deal with images in the source and target domains separately. Moreover, in practical terms, we can effortlessly get a small partial labeled images in the target scenario. Then, we can obtain considerable benefits by applying the semi-supervised learning (or called few-shot learning).

Therefore, beyond the general UDA setting, DTPL [40] proposes a weakly supervised progressive domain adaptation framework by providing image-level annotations of target domain images. UMT [13] promotes the Faster R-CNN adaptation by utilizing the unbiased Mean Teacher [26] which is initially designed for semi-supervised learning task. TRKP [31] and TDD [32] apply the knowledge distillation framework to remedy cross-domain discrepancies and perceive target-relevant features. Inspired by these principles, we construct our SSDA-YOLO in a knowledge distillation structure, apply supervised learning in the source dataset, and perform unsupervised learning in the target dataset. This combination solution forms the semi-supervised learning.

3. PRELIMINARIES AND MOTIVATION

As discussed above, most state-of-the-art DAOD methods are confined to two-stage detectors, especially the Faster R-CNN. This is largely because the Faster R-CNN provides two branches of classification and localization with clear boundaries. DA-Faster [11] takes advantage of this characteristic, and firstly proposes two representations at instance-level and image-level which are widely followed until now. Recently, one-stage detectors based DAOD methods are also considering how to extract cross-domain features with their designed adaptation components at these two levels. Besides, most DAOD methods focus on the training of one shared detection network with data from both source and target domains. This adversarial way is distressful to optimize and converge. These premises motivate us in addressing two principal challenges:

Knowledge Distillation Structure: The previous DAOD method using a single shared network to fit the cross-domain data is an adversarial process. Most of them utilize the bidirectional operator Gradient Reversal Layer (GRL) [33] which is used to realize two conflicted optimization objectives. On one hand, it acts as an identity operator for minimizing the classification error during forward training. On the other hand, it becomes a negative scalar during back-propagation for maximizing the binary-classification error and learning domain-invariant features. Distance metrics like Maximum Mean Discrepancy (MMD) [41] is usually applied to measure the domain shift and supervise the model. Despite these common settings, the more robust teacher-student framework is adopted in DAOD by recently proposed approaches [13, 31, 32]. Their distillation structures can enhance source detector to perceive objects in a target image. These methods are all based on the Faster R-CNN, and distill intermediate features based knowledge [42]. We also follow the teacher-student framework, but distill knowledge based on final response [42] of one-stage YOLOv5 detector. Although there are various model setups of teacher and student relationship [42], we choose to maintain them the identical architecture.

Cross-domain Features Extraction: In the one-stage detection framework, it has unified predictions and indistinct discrimination between classification and localization. For example, EPMDA [17] based on FCOS [2] proposes the global and center-aware discriminators to imitate image-level and instance-level features extraction. I³Net [18] based on SSD [3] designs a multi-label classifier and two domain discriminators to compensate image-level and pixel-level features. The most similar to our work are DA-YOLO [22] and MS-DAYOLO [24]. DA-YOLO based on YOLOv3 [20] proposes two adaptive modules RIA and MSIA using three domain classifiers to perform image and instance level adaptation respectively. MS-DAYOLO based on YOLOv4 [6] attaches a domain adaptation network (DAN) to the backbone to directly learn domain-invariant features in multiscale. Unlike all of them, we adopt the pseudo cross-generated images to address image-level shifts, and the Mean Teacher model to obtain target domain features at instance-level for guiding the student model training.

4. PROPOSED METHOD

Our proposed SSDA-YOLO method is based on the one-stage detector YOLOv5. It contains four main components: the Mean Teacher model with a knowledge distillation framework for guiding robust student network updating, the pseudo cross-generated training images for alleviating image-level domain differences, the updated distillation loss for remedying cross-domain discrepancy, and the novel consistency loss for further redressing cross-domain objectness bias. Details of these modules are as follows.

4.1. Definition of Terms

For the cross-domain object detection task, we have a set of source images \mathbf{I}^s annotated with totally N object bounding boxes $\mathcal{B} = \{B_j |_{j=1}^N, B_j = (x_j, y_j, w_j, h_j)\}$ and corresponding class labels $\mathcal{C} = \{C_j |_{j=1}^N, C_j \in (0, 1, \dots, c)\}$ with c object classes, and a set of unlabeled target images \mathbf{I}^t . With N_s source images \mathbf{I}^s , also the bounding box coordinates set \mathcal{B}^s and the class labels set \mathcal{C}^s , we represent the source domain as $\mathcal{D}_s = \{(\mathbf{I}_i^s, \mathcal{B}_i^s, \mathcal{C}_i^s) |_{i=1}^{N_s}\}$. Similarly, we define the target domain with N_t label invisible images as $\mathcal{D}_t = \{\mathbf{I}_i^t |_{i=1}^{N_t}\}$.

Our goal of solving the DAOD problem is to learn a model that could achieve best possible performance for the target domain with given datasets \mathcal{D}_s and \mathcal{D}_t . In particular, we employ YOLOv5 [21] as our detector backbone. Following its implementations, the loss for training a supervised model with the labeled source dataset \mathcal{D}_s can be written as:

$$\mathcal{L}_{det}(\mathbf{I}^s, \mathcal{B}^s, \mathcal{C}^s) = \mathcal{L}_{box}(\mathcal{B}^s; \mathbf{I}^s) + \mathcal{L}_{cls,obj}(\mathcal{C}^s; \mathbf{I}^s) \quad (1)$$

where \mathcal{L}_{box} is the GIoU loss for predicted bounding boxes, and $\mathcal{L}_{cls,obj}$ is the Focal loss [29] of both classification probability and objectness score calculated by binary cross entropy. We mainly introduce the unsupervised domain adaptation related to the unlabeled target domain images \mathcal{D}_t in below sections.

4.2. Mean Teacher Model

The Mean Teacher (MT) model [26] is initially proposed for semi-supervised learning in image classification. It consists of a typical knowledge distillation structure with two identical model architectures (student and teacher). For domain adaptation tasks, the student model is trained with labeled data in source domain using the gradient descent optimizer. According to the MT model setting, the teacher model is updated by the exponential moving average (EMA) weights from the student model. Specifically, supposing that weight parameters of student and teacher models are noted as \mathcal{P}_s and \mathcal{P}_t respectively, we update \mathcal{P}_t at each training batch step as following:

$$\mathcal{P}_t = \gamma \mathcal{P}_t + (1 - \gamma) \mathcal{P}_s \quad (2)$$

where γ is the exponential decay. Its reasonable value is close to 1.0, typically in the multiple-nines range: 0.99, 0.999, etc.

When applying the MT model to our cross-domain object detection task, we set the unlabeled target domain samples \mathcal{D}_t as the single input of the teacher model. We also train the student model partially on these unlabeled samples \mathbf{I}^t . During the distillation, by selecting bounding boxes with high probabilities from the teacher model predictions as pseudo labels, the student model tends to reduce variance on the target domain and enhance the model robustness. Supposing that we have the augmented target inputs $\hat{\mathbf{I}}^t$ for the teacher model and

$\bar{\mathbf{I}}^t$ for the student model from the same images \mathbf{I}^t , the inconsistency in predictions between the two models can be penalized using a distillation loss defined as below:

$$\mathcal{L}_{dis}(\hat{\mathbf{I}}^t, \bar{\mathbf{I}}^t) = \mathcal{L}_{det}(\bar{\mathbf{I}}^t, \mathcal{G}_B[\mathcal{F}_B(\hat{\mathbf{I}}^t)], \mathcal{G}_C[\mathcal{F}_C(\hat{\mathbf{I}}^t)]) \quad (3)$$

where $\mathcal{F}_B(\cdot)$ and $\mathcal{F}_C(\cdot)$ are the prediction branches from the teacher model for bounding box coordinates and object classes with high maximum category score on $\hat{\mathbf{I}}^t$ respectively. The $\mathcal{G}_B[\cdot]$ and $\mathcal{G}_C[\cdot]$ are corresponding filters. Specifically, we set the MT model to evaluation mode in each step during training, and use Non-Maximum Suppression (NMS) to filter the predicted bounding boxes sorted by object confidence with a IoU threshold τ_{box} . Then, we select out the bounding boxes with category scores higher than a threshold τ_{cls} . The final pseudo labels provide the student model *instance-level* features of the target domain.

4.3. Pseudo Training Images Generation

Although we have successfully constructed a basic distillation network, it is foreseeable that the weights updating of the student model is dominated by images \mathbf{I}^s in the source domain. In contrast, the teacher model does not touch the source images and is guided by the target domain features. We need to alleviate image-level domain differences which cause two models biased toward their monotonous image inputs. Inspired by SWDA [12] which learns domain-invariant features by weak alignment at the global scene-level using CycleGAN [34], UMT [13] and TDD [32] transfer source domain images into target-like domain, and vice versa. In this paper, we choose to generate both target-like fake source images and source-like fake target images for training. Specifically, we here adopt a more superior unpaired image translator CUT [27] for faster and more robust scene transfer. We represent the translated target-like images from source images \mathbf{I}^s as \mathbf{I}_f^s , and source-like images from target images \mathbf{I}^t as \mathbf{I}_f^t , respectively. Please note that image pairs $(\mathbf{I}^s, \mathbf{I}_f^s)$ and $(\mathbf{I}^t, \mathbf{I}_f^t)$ always appear concurrently during training.

4.4. Remedying Cross-Domain Discrepancy

After generating \mathbf{I}_f^s and \mathbf{I}_f^t , to remedy the student model with cross-domain discrepancy, we add a new supervised branch with target-like images \mathbf{I}_f^s as the input (refer the yellow flow in Fig. 1), and train them exactly the same as source images \mathbf{I}^s (refer the red flow in Fig. 1). Similar to Eqn. 1, the corresponding loss function is defined as follows:

$$\mathcal{L}_{det}^\dagger(\mathbf{I}_f^s, \mathcal{B}^s, \mathcal{C}^s) = \mathcal{L}_{box}(\mathcal{B}^s; \mathbf{I}_f^s) + \mathcal{L}_{cls,obj}(\mathcal{C}^s; \mathbf{I}_f^s) \quad (4)$$

For the teacher model, to make it learn the global image-level features of the source domain, we replace the original input target images $\hat{\mathbf{I}}^t$ with source-like fake images $\hat{\mathbf{I}}_f^t$ (refer the blue flow in Fig. 1). The unlabeled target images $\bar{\mathbf{I}}^t$ for

training the student model keep unchanging (refer the green flow in Fig. 1). Thus, we update the distillation loss in Eqn. 3 into:

$$\mathcal{L}_{dis}^{\dagger}(\hat{\mathbf{I}}_f^t, \bar{\mathbf{I}}^t) = \mathcal{L}_{det}(\bar{\mathbf{I}}^t, \mathcal{G}_B[\mathcal{F}_B(\hat{\mathbf{I}}_f^t)], \mathcal{G}_C[\mathcal{F}_C(\hat{\mathbf{I}}_f^t)]) \quad (5)$$

4.5. Consistency Loss Function

Although the source and target-like paired images $(\mathbf{I}^t, \mathbf{I}_f^t)$ fed into the student model have different scene-level data distributions, they belong to the same label space. Ideally, a rational hypothesis is that the outputs of the student model feeding with both domain images should be consistent. Therefore, to ensure that their outputs are as close as possible, we can add a new constraint to the corresponding two branches. Intuitively, we have three choices: 1) apply the intermediate supervision between corresponding feature maps; 2) apply the error constraint between final predictions; 3) combine above both strategies.

The intermediate supervision strategy is initially proposed and studied by convolutional pose machines (CPM) [43] for the single person pose estimation task. It is proven reasonable in addressing vanishing gradients in supervised training. However, we here need an UDA penalization. In other words, we do not want the intermediate features of the student model to be similar after the input of \mathbf{I}^t and \mathbf{I}_f^t , but only expect the predictions to be as consistent as possible. The intermediate supervision here may be an excessive constraint. Thus, we select the second constraint by calculating the L2 distance between two final outputs. We call it consistency loss produced as follows:

$$\mathcal{L}_{con} = \|\mathcal{L}_{det}(\mathbf{I}^s, \mathcal{B}^s, \mathcal{C}^s) - \mathcal{L}_{det}^{\dagger}(\mathbf{I}_f^s, \mathcal{B}^s, \mathcal{C}^s)\|_2 \quad (6)$$

where we can also use the L1 loss. We will analyze which one is better in our ablation studies. The consistency loss seemingly can redress cross-domain biases of objectness and classification. Its effectiveness will also be proven by experiments.

4.6. Overall Optimization

The framework of our SSDA-YOLO is shown in Fig. 1. The target-like images \mathbf{I}_f^s and source-like images \mathbf{I}_f^t are generated offline by corresponding pre-trained CUT models. During inference, we only need to adopt the finely trained student model and take the target image as the single input. Our model can be trained in an end-to-end manner by optimizing all related losses jointly. The overall loss function is written as:

$$\mathcal{L} = \mathcal{L}_{det}(\mathbf{I}^s, \mathcal{B}^s, \mathcal{C}^s) + \mathcal{L}_{det}^{\dagger}(\mathbf{I}_f^s, \mathcal{B}^s, \mathcal{C}^s) + \alpha \cdot \mathcal{L}_{dis}^{\dagger}(\hat{\mathbf{I}}_f^t, \bar{\mathbf{I}}^t) + \beta \cdot \mathcal{L}_{con} \quad (7)$$

where the α and β are the trade-off hyper-parameters, and determined by experiments.

5. EXPERIMENTS

5.1. Training Configuration

In all experiments, we choose YOLOv5 with Large parameters (YOLOv5-L) as the detector for its comparable detection accuracy with state-of-the-art object detection methods in about real-time. All training and testing images are padded and resized in shape $(960, 960, 3)$. During training, each batch consists of two pairs of images: $(\mathbf{I}^s, \mathbf{I}_f^s)$ with labels and $(\mathbf{I}^t, \mathbf{I}_f^t)$ without labels. We can set the batchsize to 10 in one 24GB GTX3090 GPU. Total epochs are 200. The γ in EMA for the teacher model is set to 0.99. In filters $\mathcal{G}_B[\cdot]$ and $\mathcal{G}_C[\cdot]$, we set the IoU threshold $\tau_{box} = 0.3$ and the category score threshold $\tau_{cls} = 0.8$. Other not mentioned settings keep consistent with the setup in YOLOv5 [21]. For the hyper-parameters in SSDA-YOLO, we set $\alpha = 0.005$ and $\beta = 2.0$ in the overall loss \mathcal{L} . And the consistency loss \mathcal{L}_{con} adopts L2 distance. These selected settings will be discussed in our ablation studies.

5.2. Transfer Experiment Design

Following DA-Faster [11] and other state-of-the-art DAOD methods, we select datasets including PascalVOC [8], Clipart1k [40], Cityscapes [44], and Foggy Cityscapes [45] to validate the effectiveness and superiority of our approach. Among them, we implement the experiment **PascalVOC**→**Clipart1k** for comparing the real to virtual adaptation, and execute the experiment **Cityscapes**→**Foggy Cityscapes** for evaluating the normal to adverse weather adaptation. Besides, to test the universality of our method in real application, we conduct the evaluation of domain adaptive behavior detection on self-made yawning datasets using various K-12 course videos. This transfer case is named **Source Classroom**→**Target Classroom**. Below are details.

5.2.1. Real to Virtual Adaptation

Datasets: Following [40, 12, 18, 13], we combine the PascalVOC 2007 and 2012 datasets (totally 16,551 images) as the source domain, and take the Clipart1k dataset as the target domain. The Clipart1k contains 1,000 images from the same 20 classes as the PascalVOC dataset, and is split equally into the training and test set. We use the labeled source training set and unlabeled target training images for adaptive training. The target test set is held out for validation. The same setup is true for the following experiments.

Results: We choose four methods SWDA [12], I³Net [18], UMT [13] and TIA [30] to compare. They are all based on the Faster R-CNN. Thus, we re-executed the Source Only¹ and Oracle² experiments using the conventional YOLOv5 (with

¹The Source Only indicates training with labeled source images and directly testing on the target data without domain adaptation.

²The Oracle indicates training and testing with labeled target images.

Table 1. The transfer results of **PascalVOC**→**Clipart1k**. The bold font means the best result. The underline font means the secondly best result.

Method	aero	bicycle	bird	boat	bottle	bus	car	cat	chair	cow	table	dog	hrs	bike	prsn	plnt	sheep	sofa	train	tv	mAP
Source Only	26.0	45.9	23.2	22.1	20.1	51.7	29.8	9.4	34.6	13.6	30.1	0.9	33.7	50.0	37.2	46.2	18.9	6.7	34.1	20.5	27.7
SWDA [12]	26.2	48.5	32.6	33.7	38.5	54.3	37.1	18.6	34.8	58.3	17.0	12.5	33.8	65.5	61.6	52.0	9.3	24.9	<u>54.1</u>	49.1	38.1
I ³ Net [18]	30.0	67.0	32.5	21.8	29.2	<u>62.5</u>	41.3	11.6	37.1	39.4	27.4	19.3	25.0	67.4	55.2	42.9	19.5	36.2	50.7	39.3	37.8
UMT [13]	39.6	59.1	32.4	35.0	45.1	61.9	48.4	7.5	46.0	67.6	21.4	29.5	48.2	<u>75.9</u>	70.5	56.7	<u>25.9</u>	28.9	39.4	43.6	44.1
TIA [30]	42.2	66.0	36.9	37.3	43.7	71.8	49.7	18.2	44.9	58.9	18.2	29.1	40.7	87.8	67.4	49.7	27.4	27.8	57.1	50.6	46.3
Oracle	33.3	47.6	43.1	38.0	24.5	82.0	57.4	22.9	48.4	49.2	37.9	46.4	41.1	54.0	73.7	39.5	36.7	19.1	53.2	52.9	45.0
Source Only*	16.5	54.5	21.2	25.8	36.3	38.7	20.8	8.8	53.7	6.3	22.0	5.7	28.4	31.0	36.1	51.5	17.0	16.9	19.9	39.0	27.5
<i>Base</i>	25.3	66.8	26.5	50.1	62.1	47.5	39.3	6.7	57.6	46.4	33.3	15.2	23.4	39.9	57.2	57.8	20.5	45.0	37.0	50.5	40.4
<i>Base_D</i>	32.2	66.1	29.5	47.7	58.0	43.6	36.5	9.5	<u>63.8</u>	47.1	<u>35.8</u>	12.4	30.3	44.9	58.4	<u>59.2</u>	24.0	37.0	39.9	52.5	41.2
<i>Base_C</i>	33.0	72.9	30.9	49.6	60.3	35.4	40.2	12.4	60.7	52.6	33.8	17.7	35.7	45.4	58.3	60.5	22.8	31.6	34.6	55.3	42.2
<i>Base_{DC}</i>	30.2	76.6	<u>33.2</u>	48.4	<u>60.7</u>	41.8	39.7	8.9	64.8	51.0	38.7	25.5	36.8	44.5	59.9	57.3	18.4	41.4	49.2	58.6	<u>44.3</u>
Oracle*	21.7	74.3	34.6	39.8	47.1	74.8	57.8	22.3	47.4	52.7	34.1	39.1	29.8	58.7	75.3	46.2	45.4	27.0	48.0	41.0	45.8

* marker). Following them, we report the average precision (AP) at IoU=0.5 of each class as well as the mean AP over all classes in Table 1 for object detection on the Clipart1k test set. Particularly, we get a mAP of 40.4 with the basic SSDA-YOLO framework *Base* by only using cross-generated fake images, yet without adding the distillation loss for remedying the discrepancy ($\alpha = 0$) or adding the consistency loss ($\beta = 0$). Then, by using the distillation loss, *Base_D* improves the mAP into 41.2. Or only adding the consistency loss, *Base_C* could obtain a mAP of 42.2. Finally, our full model *Base_{DC}* reaches 44.3 mAP on the Clipart1k test set, which is comparable with the state-of-the-art performances 44.1 in UMT [13] and 46.3 in TIA [30]. However, our one-stage model is more efficient than the two-stage Faster R-CNN used by UMT and TIA when inference.

5.2.2. Normal to Adverse Weather Adaptation

Datasets: This part, we choose the Cityscapes dataset [44] as the source domain, and the Foggy Cityscapes dataset [45] as the target domain. The Cityscapes dataset is collected from the urban street scene captured in 50 cities. We select 8 classes for the experiment according to [11]. The dataset contains 2,975 and 500 images in the train set and validation set, respectively. The Foggy Cityscapes is a synthetic foggy scene dataset from Cityscapes, which has exactly the same data split. We take the Cityscapes train set images with labels and the Foggy Cityscapes train set images without labels for training, and test on the validation set of Foggy Cityscapes.

Results: We choose methods DA-Faster [11] and eight representative methods to compare. Except [17, 16, 19] which are based on FCOS [2], the others are all based on the Faster R-CNN. Again, we have retrained and got new baselines for both Source Only and Oracle using YOLOv5 (with * marker). All results of DAOD on the Foggy Cityscapes validation set are reported in Table 2. Due to the efficient data augmentation of YOLOv5, the Source Only method achieves a comparable mAP value 35.9 to the recent state-of-the-art methods (e.g., EPMDA [17] and UMT [13]). Then, our basic method *Base* is obviously better than the Source Only method. By adding

Table 2. The transfer results of **Cityscapes**→**Foggy Cityscapes**. The bold font means the best result.

Method	Detector	bus	bicycle	car	mycle	person	rider	truck	mAP
Source Only	Faster R-CNN	24.7	29.0	27.2	16.4	24.3	31.5	9.1	21.8
DA-Faster [11]	Faster R-CNN	35.3	27.1	40.5	20.0	25.0	31.0	20.2	27.6
SWDA [12]	Faster R-CNN	36.2	35.3	43.5	30.0	29.9	42.3	32.6	34.3
NLDA [14]	Faster R-CNN	35.1	42.2	49.2	30.2	45.3	27.0	26.9	36.0
EPMDA [17]	FCOS	41.9	38.7	56.7	22.6	41.5	26.8	24.6	35.0
UMT [13]	Faster R-CNN	56.5	37.3	48.6	30.4	33.0	46.7	46.8	34.1
TIA [30]	Faster R-CNN	52.1	38.1	49.7	37.7	34.8	46.3	48.6	31.1
SIGMA [16]	FCOS	50.4	40.6	60.3	31.7	44.0	43.9	51.5	31.6
MGADA [19]	FCOS	50.7	42.8	60.6	38.3	43.9	49.6	39.0	29.6
TDD [32]	Faster R-CNN	53.0	49.1	68.2	38.9	50.7	53.7	45.1	35.1
Oracle	Faster R-CNN	50.0	36.2	49.7	34.7	33.2	45.9	37.4	35.6
Source Only*	YOLOv5-L	37.2	39.2	51.9	30.3	46.5	49.0	8.5	24.2
<i>Base</i>	YOLOv5-L	55.8	50.8	71.4	40.9	57.7	57.9	46.3	31.3
<i>Base_D</i>	YOLOv5-L	55.7	53.1	71.7	44.2	59.4	61.2	46.9	36.0
<i>Base_C</i>	YOLOv5-L	61.9	52.8	73.6	47.2	60.2	59.0	42.9	37.1
<i>Base_{DC}</i>	YOLOv5-L	63.0	53.6	74.3	47.4	60.6	62.1	48.0	37.8
Oracle*	YOLOv5-L	61.2	52.1	77.2	47.8	62.8	60.3	50.3	46.2

the distillation loss and consistency loss, our complete model *Base_{DC}* reaches a mAP of 55.9, which is much higher than so far best result 49.2 in TDD [32]. Some qualitative results are shown in Fig. 2.



(a) Oracle YOLOv5 (b) Source Only YOLOv5 (c) SSDA-YOLO

Fig. 2. Visual detection examples using the original YOLOv5 model on: (a) clear images and (b) foggy images. (c) Our proposed SSDA-YOLO applied onto foggy images.

5.2.3. Cross Classroom Yawning Detection Adaptation

Datasets: In our research of automatic teaching observation, we have collected about 1,300+ real course videos from 21 K-12 schools in the same city district. We define them as the source domain. Meanwhile, in another city, we have totally got 30 course videos from different classrooms in one high school. We deem these data as the target domain. Then, we sample these videos every three seconds to generate static frames and annotated the yawning behavior using bounding box. Finally, we totally obtain 12,924 valid images in the source school and 1,990 images in the target school. Two pairs of example images are shown in Fig. 3. We divide the data in the two domains into train set and test set with an 8 : 2 ratio, respectively.

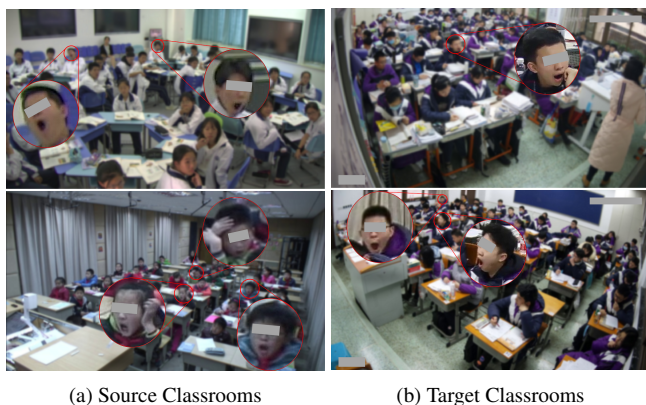


Fig. 3. Example images with yawning behaviors are from (a) Source Classrooms and (b) Target Classrooms. Images are masked to protect privacy.

Results: Since we only have one category yawning, a more stringent index $mAP^{5:.95}$ is adopted to measure the performance. Firstly, we train YOLOv5 on the train set of the source school and the target school, respectively. Then we get the results of Source Only and Oracle on the test set of the target school. Not surprisingly, as shown in Table 3, even though there are a large number of yawning images in the source school, due to the domain shifts mainly caused by different classroom scenes, the final Source Only model with 38.7 $mAP^{5:.95}$ performs rather poor compared with Oracle with 65.1 on the target test set. By using our methods *Base*, *Base_D*, *Base_C* and *Base_{DC}* in turn, the $mAP^{5:.95}$ is improved to 43.7, 46.2, 47.6 and 52.5 respectively. Although a gap still exists comparing with the Oracle result, our proposed method can alleviate the accuracy degradation distinctly of cross-domain behavior detection in real classrooms.

5.3. Ablation Studies

Although above transfer experiments have shown that each proposed module in SSDA-YOLO can improve the DAOD

Table 3. The transfer results of Source Classroom→Target Classroom.

Method	$mAP^{0.50}$	$mAP^{0.75}$	$mAP^{5:.95}$
Source Only	77.5	31.8	38.7
<i>Base</i>	77.3	43.6	43.7 (↑ 5.0)
<i>Base_D</i>	79.5	47.2	46.2 (↑ 7.5)
<i>Base_C</i>	80.4	50.7	47.6 (↑ 8.9)
<i>Base_{DC}</i>	79.5	58.8	52.5 (↑ 13.8)
Oracle	93.5	84.2	65.1

performance separately, we want to further explore the process of acquiring optimal parameters. Without loss of generality, we use YOLOv5 with Small parameters (YOLOv5-S) as the backbone, and PascalVOC→Clipart1k as the domain transfer test case. Each training is shortened to 100 epochs for simplicity.

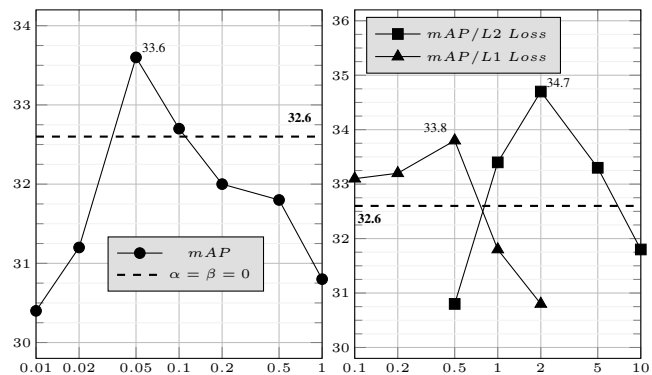


Fig. 4. The effect of α (hav- **Fig. 5.** The effect of β and $ing \times 10$.)

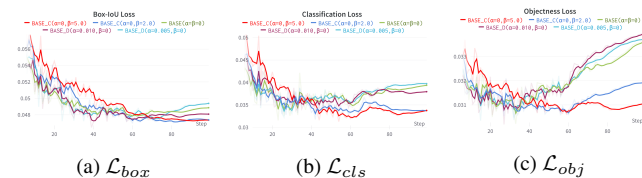


Fig. 6. Recorded loss trends when evaluating on the target domain test set. We choose three kinds of experiment setup for comparing: 1) *Base* without adding \mathcal{L}_{dis} and \mathcal{L}_{con} , 2) *Base_D* with only adding \mathcal{L}_{dis} , and 3) *Base_C* with only adding \mathcal{L}_{con} .

5.3.1. Weight α for Distillation Loss

To seek out the optimal parameter value of α , we firstly set $\beta = 0$ in total loss function, and sample α from 0.001 to 0.1 with about $2 \times$ increasing in each step. The experimental results are shown in Fig. 4. The optimal $mAP^{0.50}$ result is achieved when $\alpha = 0.005$. And a smaller or larger α will decrease the performance of distillation loss for remedying

cross-domain discrepancy. This indicates that we should not be too aggressive when adjusting the weight of distillation loss.

5.3.2. Weight β for Consistency Loss

Similarly, to seek out the best value of β , we firstly set $\alpha = 0$ and L2 loss in \mathcal{L}_{con} . We then select β from five candidates (0.5, 1.0, 2.0, 5.0, 1.0). The weight β is larger than α , which is determined by the absolute value of the corresponding loss. Then, we obtained all testing results in Fig. 5. The optimal mAP is achieved when $\beta = 2.0$. Moreover, to verify which kind of consistency loss is better, we repeat the above experiments except for selecting β from (0.1, 0.2, 0.5, 1.0, 2.0) and changing \mathcal{L}_{con} into L1 loss. As in Fig. 5, the highest mAP using L1 loss is 33.8 when $\beta = 0.5$, which is inferior to the counterpart 34.7 of L2 loss.

5.3.3. Validity of Consistency Loss

Finally, we recorded the trends of \mathcal{L}_{cls} , \mathcal{L}_{box} and \mathcal{L}_{obj} on the target domain test set before and after adding the consistency loss. As we can see in Fig. 6, the \mathcal{L}_{con} (*BaseC*) can obviously promote the convergence of all three losses, especially the healing of objectness loss \mathcal{L}_{obj} . This further intuitively shows the essential effectiveness of the proposed consistency loss \mathcal{L}_{con} .

6. CONCLUSION

In this paper, we propose a novel semi-supervised cross-domain object detection method named SSDA-YOLO. We abandon the current less efficient Faster R-CNN, which has been dominated in previous works, and introduce the more superior YOLOv5 as our backbone detector. Specifically, our framework contains three effective components. First, based on the knowledge distillation structure, we separately learn the YOLOv5 as a student network and a Mean Teacher model based teacher network to build a robust training. Next, we perform style transfer to cross-generate pseudo training images for alleviating the global domain differences. Finally, we apply a consistency loss function to correct the prediction shifts of images from different domains but with same labels. We have performed experiments on both public benchmarks and self-made yawning behavior datasets. The final results prove the effectiveness and superiority of our proposed SSDA-YOLO in real cross-domain object detection applications.

Acknowledgments

This paper is supported by NSFC (No. 62176155, 61772330), Shanghai Municipal Science and Technology Major Project (2021SHZDZX0102)

7. REFERENCES

- [1] Shaoqing Ren, Kaiming He, Ross Girshick, and Jian Sun, "Faster r-cnn: Towards real-time object detection with region proposal networks," *NIPS*, vol. 28, pp. 91–99, 2015.
- [2] Zhi Tian, Chunhua Shen, Hao Chen, and Tong He, "Fcos: Fully convolutional one-stage object detection," in *ICCV*, 2019, pp. 9627–9636.
- [3] Wei Liu, Dragomir Anguelov, Dumitru Erhan, Christian Szegedy, Scott Reed, Cheng-Yang Fu, and Alexander C Berg, "Ssd: Single shot multibox detector," in *ECCV*. Springer, 2016, pp. 21–37.
- [4] Kaiming He, Georgia Gkioxari, Piotr Dollár, and Ross Girshick, "Mask r-cnn," in *ICCV*, 2017, pp. 2961–2969.
- [5] Tsung-Yi Lin, Piotr Dollár, Ross Girshick, Kaiming He, Bharath Hariharan, and Serge Belongie, "Feature pyramid networks for object detection," in *CVPR*, 2017, pp. 2117–2125.
- [6] Alexey Bochkovskiy, Chien-Yao Wang, and Hong-Yuan Mark Liao, "Yolov4: Optimal speed and accuracy of object detection," *arXiv preprint arXiv:2004.10934*, 2020.
- [7] Zheng Ge, Songtao Liu, Feng Wang, Zeming Li, and Jian Sun, "Yolox: Exceeding yolo series in 2021," *arXiv preprint arXiv:2107.08430*, 2021.
- [8] Mark Everingham, Luc Van Gool, Christopher KI Williams, John Winn, and Andrew Zisserman, "The pascal visual object classes (voc) challenge," *IJCV*, vol. 88, no. 2, pp. 303–338, 2010.
- [9] Tsung-Yi Lin, Michael Maire, Serge Belongie, James Hays, Pietro Perona, Deva Ramanan, Piotr Dollár, and C Lawrence Zitnick, "Microsoft coco: Common objects in context," in *ECCV*. Springer, 2014, pp. 740–755.
- [10] Alina Kuznetsova, Hassan Rom, Neil Alldrin, Jasper Uijlings, Ivan Krasin, Jordi Pont-Tuset, Shahab Kamali, Stefan Popov, Matteo Mallocci, Alexander Kolesnikov, et al., "The open images dataset v4," *IJCV*, vol. 128, no. 7, pp. 1956–1981, 2020.
- [11] Yuhua Chen, Wen Li, Christos Sakaridis, Dengxin Dai, and Luc Van Gool, "Domain adaptive faster r-cnn for object detection in the wild," in *CVPR*, 2018, pp. 3339–3348.
- [12] Kuniaki Saito, Yoshitaka Ushiku, Tatsuya Harada, and Kate Saenko, "Strong-weak distribution alignment for adaptive object detection," in *CVPR*, 2019, pp. 6956–6965.

- [13] Jinhong Deng, Wen Li, Yuhua Chen, and Lixin Duan, “Unbiased mean teacher for cross-domain object detection,” in *CVPR*, 2021, pp. 4091–4101.
- [14] Mehran Khodabandeh, Arash Vahdat, Mani Ranjbar, and William G Macready, “A robust learning approach to domain adaptive object detection,” in *ICCV*, 2019, pp. 480–490.
- [15] Xingxu Yao, Sicheng Zhao, Pengfei Xu, and Jufeng Yang, “Multi-source domain adaptation for object detection,” in *ICCV*, 2021, pp. 3273–3282.
- [16] Wuyang Li, Xinyu Liu, and Yixuan Yuan, “Sigma: Semantic-complete graph matching for domain adaptive object detection,” in *CVPR*, 2022.
- [17] Cheng-Chun Hsu, Yi-Hsuan Tsai, Yen-Yu Lin, and Ming-Hsuan Yang, “Every pixel matters: Center-aware feature alignment for domain adaptive object detector,” in *ECCV*. Springer, 2020, pp. 733–748.
- [18] Chaoqi Chen, Zebiao Zheng, Yue Huang, Xinghao Ding, and Yizhou Yu, “I3net: Implicit instance-invariant network for adapting one-stage object detectors,” in *CVPR*, 2021, pp. 12576–12585.
- [19] Wenzhang Zhou, Dawei Du, Libo Zhang, Tiejian Luo, and Yanjun Wu, “Multi-granularity alignment domain adaptation for object detection,” in *CVPR*, 2022.
- [20] Joseph Redmon and Ali Farhadi, “Yolov3: An incremental improvement,” *arXiv preprint arXiv:1804.02767*, 2018.
- [21] Glenn Jocher, K Nishimura, T Mineeva, and R Vilarino, “Yolov5,” *Code repository <https://github.com/ultralytics/yolov5>*, 2020.
- [22] Shizhao Zhang, Hongya Tuo, Jian Hu, and Zhongliang Jing, “Domain adaptive yolo for one-stage cross-domain detection,” in *ACML*. PMLR, 2021, pp. 785–797.
- [23] Wenyu Liu, Gaofeng Ren, Runsheng Yu, Shi Guo, Jianke Zhu, and Lei Zhang, “Image-adaptive yolo for object detection in adverse weather conditions,” *arXiv preprint arXiv:2112.08088*, 2021.
- [24] Mazin Hnawa and Hayder Radha, “Multiscale domain adaptive yolo for cross-domain object detection,” *arXiv preprint arXiv:2106.01483*, 2021.
- [25] Vidit Vidit and Mathieu Salzmann, “Attention-based domain adaptation for single stage detectors,” *arXiv preprint arXiv:2106.07283*, 2021.
- [26] Antti Tarvainen and Harri Valpola, “Mean teachers are better role models: Weight-averaged consistency targets improve semi-supervised deep learning results,” *NIPS*, vol. 30, 2017.
- [27] Taesung Park, Alexei A Efros, Richard Zhang, and Jun-Yan Zhu, “Contrastive learning for unpaired image-to-image translation,” in *ECCV*. Springer, 2020, pp. 319–345.
- [28] Chien-Yao Wang, Hong-Yuan Mark Liao, Yueh-Hua Wu, Ping-Yang Chen, Jun-Wei Hsieh, and I-Hau Yeh, “Cspnet: A new backbone that can enhance learning capability of cnn,” in *CVPRW*, 2020, pp. 390–391.
- [29] Tsung-Yi Lin, Priya Goyal, Ross Girshick, Kaiming He, and Piotr Dollár, “Focal loss for dense object detection,” in *ICCV*, 2017, pp. 2980–2988.
- [30] Liang Zhao and Limin Wang, “Task-specific inconsistency alignment for domain adaptive object detection,” in *CVPR*, 2022.
- [31] Jiayi Wu, Jiabin Chen, Mengzhe He, Yiru Wang, Bo Li, Bingqi Ma, Weihao Gan, Wei Wu, Yali Wang, and Di Huang, “Target-relevant knowledge preservation for multi-source domain adaptive object detection,” in *CVPR*, 2022.
- [32] Mengzhe He, Yali Wang, Jiayi Wu, Yiru Wang, Hanqing Li, Bo Li, Weihao Gan, Wei Wu, and Yu Qiao, “Cross domain object detection by target-perceived dual branch distillation,” in *CVPR*, 2022.
- [33] Yaroslav Ganin, Evgeniya Ustinova, Hana Ajakan, Pascal Germain, Hugo Larochelle, François Laviolette, Mario Marchand, and Victor Lempitsky, “Domain-adversarial training of neural networks,” *JMLR*, vol. 17, no. 1, pp. 2096–2030, 2016.
- [34] Jun-Yan Zhu, Taesung Park, Phillip Isola, and Alexei A Efros, “Unpaired image-to-image translation using cycle-consistent adversarial networks,” in *ICCV*, 2017, pp. 2223–2232.
- [35] Lixin Duan, Ivor W Tsang, and Dong Xu, “Domain transfer multiple kernel learning,” *TPAMI*, vol. 34, no. 3, pp. 465–479, 2012.
- [36] Raghuraman Gopalan, Ruonan Li, and Rama Chellappa, “Domain adaptation for object recognition: An unsupervised approach,” in *ICCV*. IEEE, 2011, pp. 999–1006.
- [37] Mingsheng Long, Yue Cao, Jianmin Wang, and Michael Jordan, “Learning transferable features with deep adaptation networks,” in *ICML*. PMLR, 2015, pp. 97–105.
- [38] Yaroslav Ganin and Victor Lempitsky, “Unsupervised domain adaptation by backpropagation,” in *ICML*. PMLR, 2015, pp. 1180–1189.
- [39] Saeid Motiian, Marco Piccirilli, Donald A Adjeroh, and Gianfranco Doretto, “Unified deep supervised domain adaptation and generalization,” in *ICCV*, 2017, pp. 5715–5725.

- [40] Naoto Inoue, Ryosuke Furuta, Toshihiko Yamasaki, and Kiyoharu Aizawa, “Cross-domain weakly-supervised object detection through progressive domain adaptation,” in *CVPR*, 2018, pp. 5001–5009.
- [41] Arthur Gretton, Karsten M Borgwardt, Malte J Rasch, Bernhard Schölkopf, and Alexander Smola, “A kernel two-sample test,” *JMLR*, vol. 13, no. 1, pp. 723–773, 2012.
- [42] Jianping Gou, Baosheng Yu, Stephen J Maybank, and Dacheng Tao, “Knowledge distillation: A survey,” *IJCV*, vol. 129, no. 6, pp. 1789–1819, 2021.
- [43] Shih-En Wei, Varun Ramakrishna, Takeo Kanade, and Yaser Sheikh, “Convolutional pose machines,” in *CVPR*, 2016, pp. 4724–4732.
- [44] Marius Cordts, Mohamed Omran, Sebastian Ramos, Timo Rehfeld, Markus Enzweiler, Rodrigo Benenson, Uwe Franke, Stefan Roth, and Bernt Schiele, “The cityscapes dataset for semantic urban scene understanding,” in *CVPR*, 2016, pp. 3213–3223.
- [45] Christos Sakaridis, Dengxin Dai, and Luc Van Gool, “Semantic foggy scene understanding with synthetic data,” *IJCV*, vol. 126, no. 9, pp. 973–992, 2018.